Gold Nanoparticle Mediated Formation of Aligned Nanotube Composite Films

Jingbiao Cui,[†] Charles P. Daghlian,[‡] and Ursula J. Gibson*[,†]

Thayer School of Engineering, Dartmouth College, Hanover, New Hampshire 03755-8000, and Rippel Electron Microscope Facility, Dartmouth College, Hanover, New Hampshire 03755-7605

Received: November 17, 2004; In Final Form: April 21, 2005

We report on the formation of highly anisotropic nanotube composite materials, made by the attachment of gold nanoparticles to the surface of the single-walled carbon nanotubes, followed by preparation of an aligned composite film by compression in a Langmuir−Blodgett trough. The gold is attached in a one-step sonication procedure. The gold-modified nanotube material forms a stable suspension in toluene and has been characterized by atomic force and scanning force microscopy, energy-dispersive X-ray spectroscopy, and Raman spectroscopy. The aligned films have highly anisotropic electrical properties, with a factor of ∼3000 difference in the conductivity between the aligned and perpendicular directions.

Introduction

Since their discovery in 1991,[1] single-walled carbon nanotubes (SWCNTs) have been extensively studied due to their unique mechanical, chemical, and electrical properties and their potential applications in nanoscale electronic devices.[2] For example, nanotubes are attractive as electrical connecting wires or as active electrical elements. A parallel array of tubes, modified to show a decrease in conductivity upon exposure to a particular substance, would make a sensitive chemical detector. However, SWCNTs are difficult to separate and manipulate; they are not soluble in common solvents. Modification of the nanotube surface by covalent or noncovalent attachment of organic and inorganic groups is generally necessary to make SWCNTs soluble. The modification processes are associated with significant disruption of nanotube structures including carbon−carbon bond breaking and defect introduction on the tube wall.[3−12] Attaching such organic and inorganic groups generally requires preparation of binding sites such as hydroxyl and carboxyl groups on which the attached materials can anchor.[13−16] These binding sites can be created by processing the SWCNTs in concentrated acid.

Thiols have been used as links for metallic nanoparticle attachment to the sidewall of purified nanotubes with hydroxyl or carboxyl groups as precursors.[17−20] Recently, Han et al. attached alkanethiol-capped Au nanoparticles to multiwalled carbon nanotubes, ascribing the binding to a combination of hydrophobic and hydrogen-bonding interactions between the capping shell and the nanotube surface.[21] We have demonstrated that pure alkanethiols can interact directly with the side wall of as-grown nanotubes, resulting in solubility of SWCNTs in toluene, with a concomitant change in the transport properties of the tubes.[22] The ability to modify the tubes using a variety of methods is critical for constructing more complex materials from them; the metal particles can serve as intermediaries for attaching other species of interest. In addition, the attached metallic nanoparticles are visible by a number of methods and may be useful in identifying the locations of defects or chemical reaction sites on the tube wall.

Here we report on a simple one-step method to attach dodecanethiol-stabilized Au nanoparticles onto the sidewall of as-grown SWCNTs, resulting in solubility of the modified tubes in toluene. The advantages of the method reported here include room temperature (acid free) treatment in a common solvent, full length modification, and removal of the requirement for preintroduced binding sites. The decoration results in reduced tangling of the nanotubes and permits assembly of preferentially oriented monolayer films using a Langmuir−Blodgett tank. The anisotropy is noticeable in scanning electron micrographs and is quite pronounced in electrical transport measurements. Although only gold nanoparticles were used in this study, the method could be easily extended to attach other metallic nanoparticles to the sidewall of nanotubes. While we used the modification as a means to an end, there is a fundamental mechanism involved that can be applied to a wider variety of problems—that thiols of different kinds can be attached directly to the sidewalls of nanotubes and that the nature of the attached moieties controls the residual interactions between the tubes. Thus, solubility can be imparted to the nanotubes by separating them with short-chain alkane thiols, but using larger additions, such as gold nanoparticles can be used to reduce interactions sufficiently to allow alignment under compression.

Experimental Section

SWCNT raw materials were purchased from Carbolex, Inc., Lexington, KY (prepared by arc discharge).[1] All the experimental data reported here were obtained using the as-grown nanotubes without any treatment or purification. Dodecanethiol stabilized Au nanoparticles with core sizes of ∼2 nm were synthesized by following the procedure of Hostetler et al.[23] Solutions of the gold nanoparticles were prepared in toluene at concentrations of 0.01−0.5 μM, in 5 mL aliquots and about 100 μg of SWCNTs were added to each. The vials containing nanotubes were sonicated using a Branson Ultrasound Cleaner (B-221). The bulk nanotubes become dispersed and gradually dissolved in the mixtures containing Au nanoparticles with a color change from pink to gray. After sonication for 1−3 h, a homogeneous nanotube suspension was obtained. The solutions

* To whom correspondence should be addressed. E-mail: u.gibson@dartmouth.edu.
[†] Thayer School of Engineering.
[‡] Rippel Electron Microscope Facility.

10.1021/jp044762i CCC: $30.25
Published on Web 05/19/2005

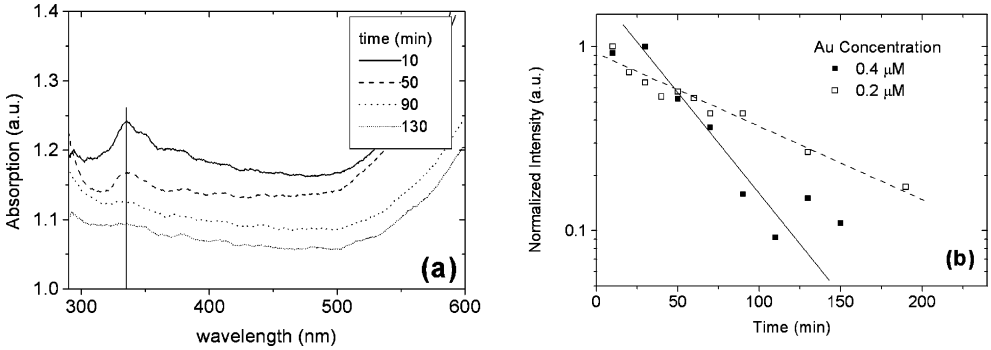

Figure 1. (a) UV−vis absorption spectra of SWCNTs in toluene that contains dodecanethiol stabilized Au nanoparticles. The vertical line indicates the position of the absorption peak. The gold nanoparticle solution was used as the baseline for the absorption measurements, so the plasma resonance peak does not appear in the spectra. (b) Integrated absorption intensity at 335 nm as a function of sonication time. The solid and open squares represent two sets of experimental data which were obtained with high (∼0.4 μM) and low Au concentration (∼0.2 μM) in toluene. The solid and dash lines are fits to the experimental data using eq 1 with time constants of 26 and 50 min, respectively.

were stored at room temperature and showed no aggregation after more than 3 months.

The UV−vis absorption spectrum of the nanotube solution was measured using a quartz cuvette and an Ocean Optics Spectrometer (USB 2000) at 10−20 min intervals during sonication. The absorption spectrum of the gold nanoparticle solution was taken as a reference, and subsequent spectra were divided by this reference.

The modified nanotubes were investigated by an atomic force microscopy (AFM, Digital Nanoscope Dimension 3100) in tapping mode at room temperature and by high-resolution scanning electron microscopy (SEM) in an XL-30 from FEI. Samples for the microscopy and Raman work were prepared by depositing a 10−20 μL drop of the solution onto a silicon substrate and allowing it to dry. Raman spectroscopy was performed at room temperature with an excitation wavelength of 532 nm in a Thermo Nicolet Almega confocal Raman microscope.

Aligned layers of the nanotubes were prepared using a Langmuir−Blodgett tank. The films were prepared by stepwise (5, 15, 25, 40 mN/n) increases in the surface pressure on the tank. After each compression step, the surface was allowed to relax for 30 min. Films with preferential orientation were transferred onto oxidized silicon wafers in a horizontal geometry to minimize disturbance of the water surface during transfer.

Electrical transport measurements were performed at room temperature using a Keithley 236 source-measure unit. Gold electrodes with a separation of 30 μm were defined on an oxidized silicon wafer using standard photolithography and a liftoff process. The nanotubes were deposited on top of the electrodes by the Langmiur−Blodgett technique described above. Electrode gaps both parallel to and perpendicular to the alignment direction introduced by the compression process allowed characterization of the anisotropy.

Results and Discussion

Gold Nanoparticle Modification of Nanotubes. Sonication of the bulk nanotubes for short times (less than 45 min) resulted in partial dispersion of the nanotubes with material settling out after less than 15 min. After continued sonication (more than 90 min), the Au nanoparticle/nanotube solution became completely homogeneous and was stable for several months. This solubility change was associated with changes in the optical, Raman, and electrical properties of the nanotubes.

The UV−vis spectrum showed an absorption peak at 335 nm for the initial nanotube suspensions in the Au nanoparticle/toluene solution. The intensity of this absorption peak gradually decreased with increased sonication time; this was also observed for nanotube dissolution using mixtures of dodecanethiol and toluene.[22] The absence of solubility in sonicated *dodecane*/toluene mixtures[22] indicates direct sulfur interaction with the nanotubes. Figure 1a displays the absorption spectrum as a function of time for a nanoparticle/nanotube solution. Because of the strong, and rapidly changing, absorption of the gold nanoparticles in the region of interest, we used a reference solution which has the same concentration of gold nanoparticles as the test sample. This makes the change due to the nanotubes easier to evaluate; rather than a small feature on a sloping background, the absorption appears as a distinct peak. The plasma resonance feature is also divided out and thus does not appear in the spectrum. Figure 1b shows the measured absorption at 335 nm as a function of sonication time for two different Au nanoparticle concentrations. The solid and dashed lines are fits to the experimental data by a first-order exponential decay. Both absorption intensities show reasonable agreement with exponential behavior. Higher Au nanoparticle concentration in toluene (solid squares) resulted in a faster decrease in the absorption intensity as well as faster stabilization of the nanotube suspensions. Mixtures with gold nanoparticles became stable more rapidly than solutions with only dodecanethiol/toluene, suggesting that the particles drive the reaction faster either by nucleating cavitation or by momentum transfer.

The intensity of the absorption peak at 335 nm is directly associated with the solubility of SWCNTs in toluene. It may result from π plasmon absorption[24] or possibly light scattering of bundled nanotubes. As the tubes dissociate from one another, the dimension reduction leads to a disappearance of this characteristic peak.

The nanotubes dissolved in toluene were found to have Au nanoparticles attached to the sidewall. A typical AFM image of sonicated nanotubes deposited on a silicon substrate is shown in Figure 2. Nanotubes with lengths up to 6 μm were observed in AFM and the nanotube surface was covered with protrusions which were confirmed by SEM to be Au nanoparticles. The height of the modified nanotube is about 8 nm, larger than our measured values of 1−3 nm for single nanotubes or small bundles. Assuming the nanotubes with diameter of 1.5 nm are fully covered by one layer of Au nanoparticles of 3 nm (including ligand shells), then the decorated nanotubes should have heights of about 7.5 nm. This value agrees well with the typical height of the modified nanotubes. Due to the poor lateral resolution of AFM, it is difficult to detect individual nanoparticles on nanotubes. Therefore, each bump in Figure 2 may

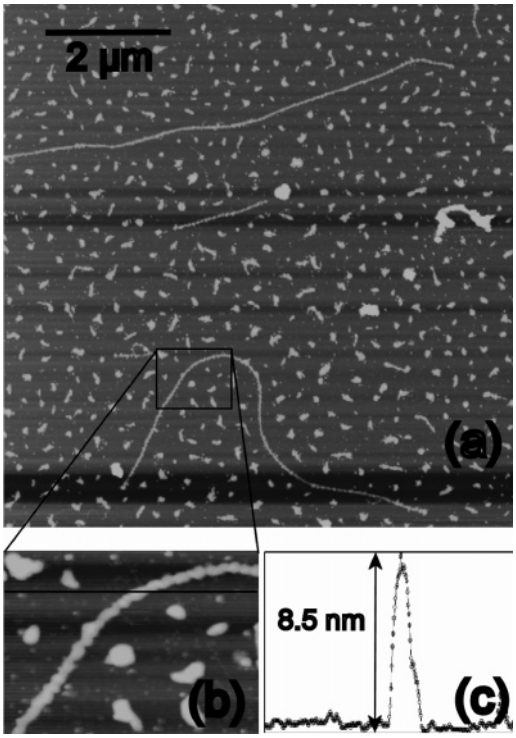

Figure 2. (a) AFM images of Au-decorated SWCNTs on a silicon substrate; (b) AFM image with higher magnification; (c) a profile across the nanotubes as indicated by a horizontal line in b.

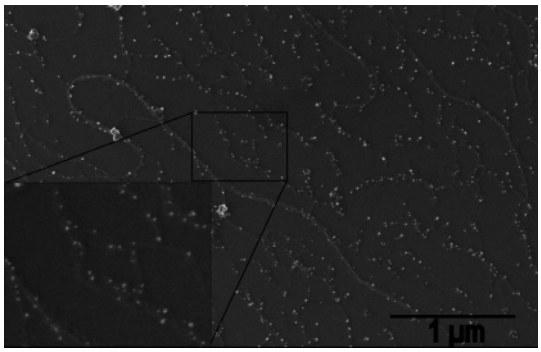

Figure 3. SEM image of Au nanoparticle decorated SWCNTs on Si substrate, after solvent rinse. The inset is an image with high magnification. The bright spots along the nanotubes are Au nanoparticles.

not represent exactly one Au particle. Note that some free Au nanoparticles in the solution were deposited as aggregates on the substrate between the nanotubes. It was possible to remove most of these aggregates using a 30/70 mixture (by volume) of methanol and toluene; this was done prior to imaging in the SEM.

The Au nanoparticles on the SWCNTs were directly observed by high-resolution SEM. Figure 3 shows an SEM image taken on a nanotube sample that was sonicated for 120 min before drop-casting onto a silicon substrate. The gold nanoparticle concentration used during sonication was 0.1 μM, and the sample was rinsed with the methanol/toluene mixture to remove excess nanoparticle aggregates prior to the SEM measurements. The inset of Figure 3 is an SEM image with higher magnification, which clearly indicates that the nanoparticles are associated with nanotubes. The average distance between the attached nanoparticles is about 50−100 nm. The increased separation of the nanoparticles over that observed in the AFM sample may be due to the washing process removing weakly bound particles.

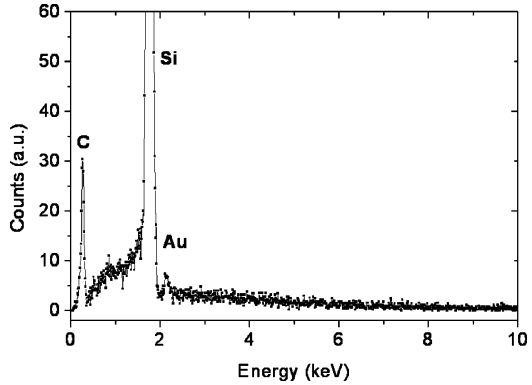

Figure 4. EDX spectrum of Au nanoparticle decorated SWCNTs on silicon.

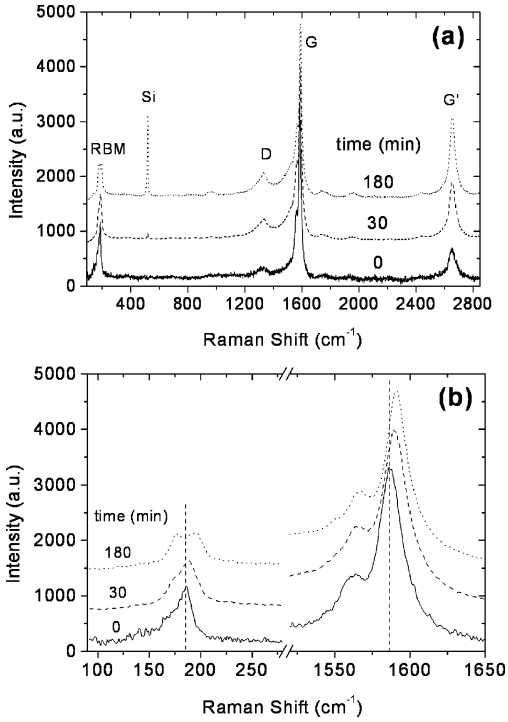

Figure 5. (a) Raman spectra of nanotubes sonicated in the gold nanoparticle/toluene solution for different times as denoted in the figure. (b) Details of RBM and G modes. The vertical lines indicate the peak positions of RBM at 186 cm^{-1} and G modes at 1586 cm^{-1} for the as-grown nanotubes. The spectra were offset vertically for clarity. The intensities were normalized to the G mode peak.

The bright spots in the SEM image were tentatively identified as Au nanoparticles since gold has a higher secondary electron emission efficiency than either silicon or carbon. This was confirmed by the energy-dispersive X-ray spectroscopy (EDX) measurement as shown in Figure 4. In addition to the strong signal from the silicon substrate, both Au and carbon were detected by EDX. A line scan over the particles unambiguously identifies the gold.

Figure 5 shows Raman spectra taken on nanotubes after they were sonicated for 0, 30, and 180 min and dried on a silicon substrate. The intensity was normalized to the main peak around 1590 cm^{-1} so that the intensities in different spectra could be compared. As denoted in Figure 5, the most important features in SWCNT Raman spectra[25] such as the radial breathing mode (RBM) around 185 cm^{-1}, tangential G mode around 1590 cm^{-1}, the disorder induced D band around 1330 cm^{-1}, and its second-order harmonic (the G′ band) at 2655 cm^{-1} were observed in all of our nanotube samples.

Compared with the as-grown nanotubes (sonication for 0 min), two noticeable changes in both peak position and relative intensity can be seen in the Raman spectra for the modified nanotubes. Both the D and G′ band intensities are higher for the nanotubes sonicated for 30 min than for the as-grown nanotubes. Further sonication of the nanotube solution (up to 180 min) resulted in even stronger D and G′ band intensities.

These two bands correspond to disordered structures in carbon nanotubes;[25] the increase in their intensity reflects the rise in the defect density in the nanotubes. Raman measurements on dodecanethiol modified nanotubes, in the absence of gold nanoparticles, exhibited changes in Raman intensity and peak shift similar to those shown in Figure 5, strongly suggesting that it is the thiol that introduces defects and/or structural deformation in the tube wall via direct attachment. The gold particles served to accelerate this interaction. Increased concentrations of gold nanoparticles reduce the sonication time required to create a given Raman defect site intensity but are not directly correlated with increased attachment of nanoparticles. The mechanism behind the Au nanoparticle attachment may be either a mixture of hydrophobic and hydrogen-bonding interactions[21] or an exchange reaction between the thiol shell and the tube wall. In the former case, the alkane chain of the thiol ligand shell may anchor on defect sites which are created by the sonication. For the second case, the thiols are assumed to react directly with tube wall and form strong C−S bonds.[26] The Au nanoparticles are then affixed to the nanotubes by entanglement between thiols attached to the nanotubes and those attached to the nanoparticles. Further investigation is needed to clarify the mechanism behind the Au nanoparticle attachment, but sonication of nanotubes with dodecane does not result in solubility, favoring the second explanation (direct sulfur bonding).

The changes in the details for both RBM and D modes are displayed in Figure 5b. The peak position of the G mode is at 1586 cm^{-1} for the as-grown nanotubes and shifts to 1591 cm^{-1} for the modified nanotubes without a noticeable change in line shape. Peaks at 176 and 185 cm^{-1} are observed in the as-grown SWCNTs. After sonication of the nanotube solution for 180 min, the peak at 185 cm^{-1} is suppressed and gradually shifts to 195 cm^{-1}, while the one at 176 cm^{-1} shows no obvious shift. Due to the peak position shift, splitting of RMB peak becomes easy to distinguish.

The peak shifts in the Raman spectra are consistent with a separation of bundles into individual tubes, since the Raman mode frequencies for individual SWCNTs are higher than those for big bundles due to van der Waals interaction between nanotubes in the bundles.[27] It is unclear why the peak at 176 cm^{-1} showed little shift after the nanotubes were dissolved in toluene; it may indicate differential reaction rates for tubes of differing chirality or diameter. The suppression of the intensity of the RBM that does shift (from 185 to 195 cm^{-1}) is likely associated with the increasing disorder of the tubes.

Nanoparticle/Nanotube Films. Alignment of SWCNTs has been a significant challenge for applications in nanoelectronics. The extremely high aspect ratio of the tubes and ready formation of aggregates are the two main factors that make alignment difficult. Covering the surface with the thiol-passivated gold nanoparticles, which limit nanotube interaction and potentially stiffen the nanotubes due to steric interactions, could reduce clustering and aggregation of SWCNTs. We have deposited highly anisotropic monolayers of the modified tubes by the Langmuir−Blodgett (L−B) technique. Figure 6 shows AFM images of nanotube samples transferred before and after surface compression in the L−B trough. After spreading on the trough surface, the modified nanotubes are randomly distributed between islands of excess Au nanoparticles. Complete compression of the material on the water surface causes the formation of a monolayer of nanotube/nanoparticle composite material. This film has a preferential orientation perpendicular to the compression direction (see Figure 6b). For imaging purposes, the sample was washed by a mixture of methanol and toluene to remove free Au nanoparticles. The inset of Figure 6b is a Fourier transform of the image, showing distinct preferential orientation.

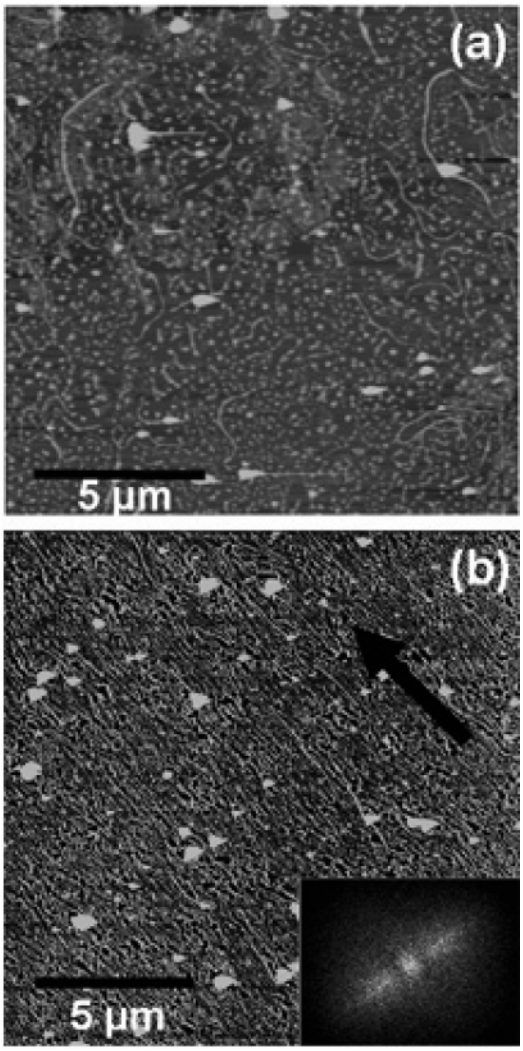

Figure 6. AFM images showing the alignment evolution of SWCNTs deposited on Si by Langmuir−Blodgett technique. The nanotubes were transferred onto Si/SiO_2 substrate (a) without surface compression and (b) with full compression. The image was obtained after removal of the excess Au nanoparticles with a mixture of methanol and toluene. The inset in lower right corner of b displays a Fourier transform of the imaged area, showing the anisotropy. The arrow in b indicates the orientation of the long axis of the nanotubes, parallel to the compression barriers.

The attached Au nanoparticles play an important role in the nanotube alignment; attempts to make textured films with dodecanethiol-modified nanotubes were unsuccessful. A similar result is obtained in the absence of nanotubes—while a uniform monolayer of thiolated Au nanoparticles can be formed in the L−B trough,[28] only aggregates of dodecanethiol were observed in our experiments. The nanoparticles seem to organize the thiols

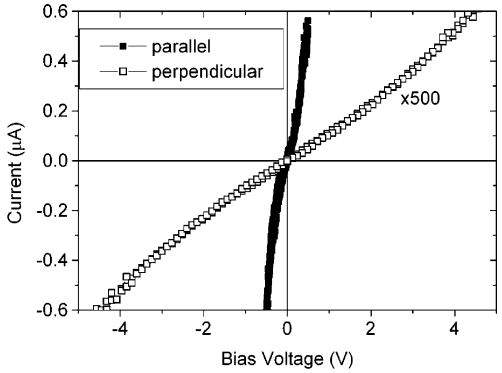

Figure 7. Current−voltage curves of aligned SWCNT monolayers measured both parallel (solid squares) and perpendicular (open squares) to the long axis of the nanotubes.

in a confirmation that limits tangling, and excess particles on the surface may serve in a lubricant role as the nanotubes are compressed.

Anisotropy in the electrical transport properties of the textured nanoparticle/nanotube monolayers was investigated. Figure 7 displays typical current−voltage ($I-V$) curves measured parallel (solid squares) and perpendicular (dash squares) to the direction of the preferential alignment of the nanotubes. The conductance parallel to the alignment direction is more than 3 orders of magnitude higher than that perpendicular to that direction. This ratio is much higher than the value (24) reported for nanotubes aligned in magnetic fields.[29]

A simple analysis can be made, on the basis of the assumption that resistive junctions between tubes dominate the impedance and that all junctions are equally resistive. For a perfectly aligned layer, the ratio of the length to width of the tubes would then equal the ratio of the conductivities. For our tubes, this ratio is approximately 5 μm/1.5 nm ($\sim$3300), on the basis of AFM observations. While the model is trivial, the calculated value is consistent with our electrical measurements.

Conclusion

In summary, as-grown single-walled carbon nanotubes were modified by sonication in a toluene-based solution of dodecanethiol stabilized gold nanoparticles. This straightforward method functionalized and dissolved SWCNTs of full length in a nonpolar solvent. The gold nanoparticles that were attached to the sidewalls of nanotubes were directly observed by SEM and AFM. Raman spectroscopy confirmed that the nanotubes were separated from each other and dissolved in toluene. The Raman intensity change (D and G′ bands) indicated that the sidewalls of SWCNTs were deformed or disrupted due to the attachment of thiol groups by which the gold nanoparticles were affixed. We have demonstrated that the nanoparticle modified nanotubes can be aligned in a Langmuir−Blodgett trough due to reduced aggregation in the presence of the nanoparticles. Anisotropy of greater than 3 orders of magnitude in the conductance has been observed in the aligned nanotube monolayers. This suggests the possibility of aligning carbon nanotubes using nanoparticles as enabling materials and has important ramifications for applications in nanotube based electronics, where large-scale alignment of nanotubes is required to avoid short circuits and undesired nanotube interconnection. This simple technique for attaching metal nanoparticles onto SWCNTs may be useful for fabricating one-dimensional nanoparticle arrays for applications in plasmonics. We observed that hexanethiol stabilized Au nanoparticles can also help dissolve SWCNTs in toluene effectively. This method can be readily extended to prepare nanocomposites using other thiol compounds, or containing different metallic nanoparticles useful for fabricating sensors and catalysts.

Acknowledgment. We thank Prof. Benjamin C. Bostick for his help with the Raman spectroscopy measurements.

References and Notes

(1) Iijima, S. *Nature* **1991**, *354*, 56−58.
(2) Dekker, C. *Phys. Today* **1999**, *52*, 22−29.
(3) Riggs, J. E.; Walker, D. B.; Carroll, D. L.; Sun, Y. P. *J. Phys. Chem. B* **2000**, *104*, 7071−7076.
(4) Chen, J.; Rao, A. M.; Lyuksyutov, S.; Itkis, M. E.; Hamon, M. A.; Haddon, R. C. *J. Phys. Chem. B* **2001**, *105*, 2525−2528.
(5) Bahr, J. L.; Tour, J. M. *J. Mater. Chem.* **2002**, *12*, 1952−1958.
(6) Star, A.; Steurman, D. W.; Heath, J. R.; Stoddart, J. F. *Angew. Chem., Int. Ed.* **2002**, *41*, 2508−2512.
(7) Niyogi, S.; Hamon, M. A.; Hu, H.; Zhao, B.; Bhowmik, P.; Sen, R, M. E. Itkis, R. Haddon, C. *Acc. Chem. Res.* **2002**, *35*, 1105−1113.
(8) Jin, Z.; Sun, X.; Xu, G.; Goh, S. H.; Ji, W. *Chem. Phys. Lett.* **2000**, *318*, 505−510.
(9) Banerjee, S.; Wong, S. S. *J. Am. Chem. Soc.* **2002**, *124*, 8940−8948.
(10) Pompeo, F.; Resasco, D. E. *Nano Lett.* **2002**, *2*, 369−373.
(11) Zhou, B.; Lin, Y.; Li, H. P.; Huang, W. J.; Connell, J. W.; Allard, L. F.; Sun, y. P. *J. Phys. Chem. B* **2003**, *107*, 13588−13592.
(12) Nakashima, N.; Tomonari, Y.; Murakami, H. *Chem. Lett.* **2002**, 638−639.
(13) Liu, J.; Rinzler, A. G.; Dai, H. J.; Hafner, J. H.; Bradley, R. K.; Boul, P. J.; Lu, A.; Iverson, R.; Shelimov, K.; Huffman, C. B.; Rodriguez-Macias, F.; Shon, Y. S.; Lee, R. R.; Colbert, D. T.; Smalley, R. E. *Science* **1998**, *280*, 1253−1256.
(14) Li, Y.; Xu, C.; Wei, B.; Zhang, X.; Zheng, M.; Wu, D.; Ajayan, P. M. *Chem. Mater.* **2002**, *14*, 483−485.
(15) Hu, H.; Bhowmik, P.; Zhao, B.; Hamon, M. A.; Itkis, M. E.; Haddon, R. C. *Chem Phys. Lett.* **2001**, *345*, 25−28.
(16) Fan, Y. W.; Burghard, M.; Klaus, K. *Adv. Mater.* **2002**, *14*, 130−133.
(17) Carillo, A.; Swartz, J. A.; Gamba, J. M.; Kane, R. S.; Chakrapani, N.; Wei, B. Q.; Ajaya, P. M. *Nano lett.* **2003**, *3*, 1437−1440.
(18) Jiang, K. Y.; Eitan, A.; Schadler, L. S.; Ajayan, P. M.; Siegel, R. W.; Grobert, N.; Mayne, M.; Reyes-Reyes, M.; Terrones, H.; Terrones, M. *Nano Lett.* **2003**, *3*, 275−277.
(19) Banerjee, I. A.; Yu, L.; Matsui, H. *Nano Lett.* **2003**, *3*, 283−287.
(20) Satishkumar, B. C.; Vogl, E. M.; Govindaraj, A.; Rao, C. N. R. *J. Phys. D: Appl. Phys.* **1996**, *29*, 3173−3176.
(21) Han, L.; Wu, W.; Kirk, F. L.; Luo, J.; Maye, M. M.; Kariuki, N. N.; Lin, Y. H.; Wang, C. M.; Zhong, C. J. *Langmuir* **2004**, *20*, 6019−6025.
(22) Cui, J. B.; Daglian, C. P.; Gibson, U. J. *J. Appl. Phys.*, submitted for publication.
(23) Hostetler, M. J.; Stokes, J. J.; Murray, R. W. *Langmuir* **1996**, *12*, 3604−3612.
(24) Shyu, F. L.; Lin, M. F. *Phys. Rev. B* **1999**, *60*, 14434−14440.
(25) Dresselhaus, M. S.; Dresselhaus, G.; Jorio, A.; Souza Filho, A. G.; Saito, R. *Carbon* **2002**, *40*, 2043.
(26) Mixteco-Sanchez, J. C.; Guirado-Lopez, R. A. *Phys. Rev. A* **2003**, *68*, 053204.
(27) Rao, A. M.; Chen, J.; Richter, E.; Schlecht, U.; Eklund, P. C.; Haddon, R. C.; Venkateswaran, U. D.; Kwon, Y.-K.; Tomanek, D. *Phys. Rev. Lett.* **2001**, *86*, 3895−3898.
(28) Brown, J. J.; Porter, J. A.; Daghlian, C. P.; Gibson, U. J. *Langmuir* **2001**, *17*, 7966−7969.
(29) Hone, J.; Llaguno, M. C.; Nemes, N. M.; Johnson, A. T.; Fischer, J. E.; Walters, D. A. *Appl. Phys. Lett.* **2000**, *77*, 666−668.